Yuriy D. KOVALEV[1], Paweł FALAT[2], Lidiya M. TYMOSHENKO[3], Kornel WARWAS[2], Ruslana ZIUBINA[2]

Opiekun naukowy: Borys E. PANCHENKO[50]

SKOŚNO-SYMETRYCZNY STAN OBCIĄŻENIA POWŁOK CIENKOŚCIENNYCH O SKOŃCZONEJ DŁUGOŚCI Z MIESZANYMI WARUNKAMI BRZEGOWYMI W PODPORACH

Streszczenie: W niniejszym artykule, zaproponowano uogólnienie metody, opracowanej uprzednio przez jednego z autorów, na klasę problemów skośno-symetrycznych stanu obciążenia powłok cienkościennych z przesuwnymi uszczelnieniami na ich brzegach. Tak zdefiniowany problem brzegowy został zredukowany do układu nieskończonego równań całkowych pojedynczych, drugiego rodzaju. Zaproponowano efektywną metodę numeryczno-analityczną do obliczenia naprężeń w powłokach. Wyniki przeprowadzanych badan zostały zilustrowane graficznie. Okazało się, że wzrost względnych naprężeń obwodowych zachodzi wraz ze zmniejszaniem się grubości powłoki kołowej, ponadto wzrasta między centralna odległość pomiędzy wewnętrzną oraz zewnętrzna powierzchnią cylindryczną, wzrasta także eliptyczność wewnętrznej powierzchni cylindrycznej.

Słowa kluczowe: równania całkowe (z całkami pojedynczymi), stan skośno-symetryczny, stan obciążenia, powłoki cienkościenne

SKEW-SYMMETRIC ELASTICITY PROBLEM FOR A THICK-WALLED SHELL OF FINITE LENGTH WITH MIXED BOUNDARY CONDITIONS ON ITS BASES

Summary: In the present paper, a method proposed by one of the authors is extended to a class of skew-symmetric problems of the stressed state of a thick-walled shell with a sliding sealing of its ends. The given boundary value problem is reduced to an infinite system of singular integral equations of the second kind. An effective numerical-analytical method is proposed to compute the stresses in shells. The results of these investigations are illustrated graphically. It is found that a growth of the relative circumferential stress occurs as the circle shell thickness decrease, the intercentral distance between inner and outer cylindrical surfaces increases and the ellipticity of an inner cylindrical surface increases.

Keywords: Singular integral equations, skew-symmetric state, stressed state, thick-walled shell

---

[50] Department of Information technologies, Odessa National Academy of Telecommunications, Kuznechna St, 65029 Odesa, Ukraine
[2] Department of Computer Science and Automatics, University of Bielsko-Biala, University of Bielsko-Biala, 2 Willowa St, 43-309 Bielsko-Biala, Poland
[3] Department of Computer Science and Management Information Systems Protection, Odessa National Polytechnic University, 1 Boulevard of Shevchenko, 65044 Odesa, Ukraine

1. Introduction

The problem of stress concentration in modern mechanical engineering is highly relevant because it is related to reliability and durability of the designed structures, as well as elements of such structures. Stress raisers in structures can occur as a result of material composition imperfections (cavities, flaws, foreign inclusions) or they can be caused by technological and structural needs (holes, cuts, etc.). In both cases, analyzing the effect of single and multiple stress raisers, as well as their mutual effect on a state of stress of structural components is very important. The accurate analysis of stress states in machine components and structural elements near stress raisers demands a three – dimensional problem statement [2, 3, 18÷22].

An effective method of solving three-dimensional problems for the layer (cylinder) is the A.I. Lurie's method of homogeneous solutions (HSM) [17]. With this method the problem of the stressed state of a layer weakened by stress raisers have been considered [10, 13]. Another effective method for the three-dimensional problems for a layer is the eigen-vector function method. This method has been employed for solving Kirsch's problem for an elastic layer [12]. Another approach to solving the problem of the stressed state of thick-walled orthotropic cylinders on the basis of three-dimensional equations of elasticity theory proposed by [11]. The HSM is efficient in the construction of a set of partial solutions for the layer (cylinder) having any boundary conditions on its bases. In the case of the mixed on the layer bases (sliding fixed ends or the bases are covered with diaphragms that are absolutely rigid in their planes and are flexible in out-of-plane direction [15]), the resulting boundary value problem becomes somewhat simpler. Such problems are also called periodic with respect to one of the coordinates. The procedure for solving such periodic problems of the theory of elasticity and electroelasticity for a piecewise homogeneous cylinder, different from Lur'ye's approach was proposed by [5], where a set of symmetric (with respect to the middle surface) problems of the theory of elasticity and electroelasticity has been solved. By using the above approach, some skew-symmetric problems of the theory of elasticity for a layer with sliding fixed ends and weakened by one stress raiser have been solved by [6, 14]. The stress analysis of stretching and bending of layers having homogeneous boundary conditions with respect to stresses on the layer bases and weakened by through-thickness cracks (cuts) has been considered by [7, 8].

The symmetric boundary value problem of the stress analysis for an equilibrium of layer with end-supports covered by diaphragms and weakened by several loaded stress raisers has been investigated by [9].

In this paper, the thick-walled isotropic shell of finite length is considered. A distinctive feature of the present investigation lies in the fact that the homogeneous solutions are constructed with the use of the procedure proposed by one of the authors [5], without invoking the very tedious Lur'ye's symbolic method. Furthermore, one-dimensional singular integral equations [16] or more precisely, an infinite system of such equations are used for solving the three-dimensional boundary value problem for a cylindrical body.

The conducted numerical investigations have shown a rapid convergence of the solution of the system of singular integral equations throughout the entire range of the "thickness" coordinate. Thus the proposed procedure actually reduces the involved boundary value problem dimensionality by two.

2. Problem statement and method of solution

Let us consider the thick-walled isotropic shell of finite length $-h \le x_3 \le h$, which cylindrical surface directrices are sufficiently smooth contours (Fig. 1).

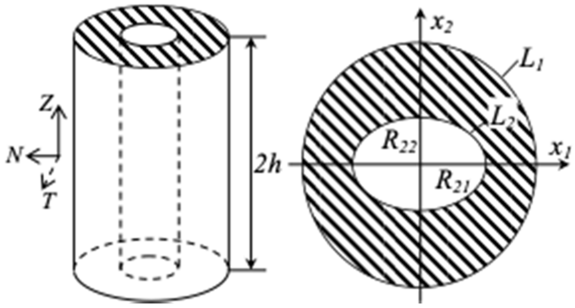

Figure 1. The thick-wall isotropic cylindrical shell of finite length

Let a surface load (N, T, Z) be applied on the cylindrical surfaces of the shell. We assume that the components of the given loading are expanded into Fourier series in the x_3 coordinate on $[-h,h]$. Let the following conditions hold on the shell ends:

$$u_3(x_1, x_2, \pm h) = \sigma_{13}(x_1, x_2, \pm h) = \sigma_{23}(x_1, x_2, \pm h) = 0 \qquad (1)$$

The components of the displacement vector can be written in the form:

$$\begin{aligned} u_i &= \sum_{k=0}^{\infty} u_{ik}(x_1, x_2) \sin \gamma_k x_3, \\ u_3 &= \sum_{k=0}^{\infty} u_{3k}(x_1, x_2) \cos \gamma_k x_3, \end{aligned} \qquad (2)$$

where $i = 1, 2$ and $\gamma_k = (2k+1)\pi/(2h)$. The above representations of the displacement vector satisfy automatically conditions (1) on the ends of the shell.
After separating the variables in the Lame equations, we have obtained the following system of equations:

$$\begin{aligned} &\kappa_k u_{ik} + \sigma \partial_i \theta_k = 0, \\ &\kappa_k u_{3k} + \sigma \gamma_k \theta_k = 0, \\ &\kappa_k = \Delta - \gamma_k^2, \ \Delta = \partial_1^2 + \partial_2^2, \\ &\theta_k = \partial_1 u_{1k} + \partial_2 u_{2k} - \gamma_k u_{3k}, \\ &\partial_i = \partial / \partial x_i, \ i=1,2, \ \sigma = (1 - 2\nu)^{-1}, \end{aligned} \qquad (3)$$

which can be integrated in the following manner. Taking into account that θ_k is a metaharmonic function, we introduce an arbitrary solution to the equation $\kappa_k^2 \psi_k = 0$ and put $\theta_k = \kappa_k \psi_k$. This provides a way to obtain the following:

$$\begin{aligned} u_{1k} &= -\sigma\partial_1\psi_k + \sigma\partial_2\varphi_k \\ u_{2k} &= -\sigma\partial_2\psi_k - \sigma\partial_1\varphi_k \\ u_{3k} &= -\gamma_k\sigma\psi_k + \Phi_k \\ \kappa_k\,\varphi_k &= 0,\ \kappa_k\Phi_k = 0, \quad (k = 0,1,...) \end{aligned} \tag{4}$$

where φ_k, Φ_k are arbitrary metaharmonic functions. Then we require that the expressions (4) satisfy the equality $\theta_k = \kappa_k\psi_k$. This leads to the following representations:

$$\begin{aligned} u_{1k} - iu_{2k} &= 2\sigma\frac{\partial}{\partial z}\left(i\varphi_k - \psi_k\right) \\ u_{3k} &= -\left(\frac{1+\sigma}{\gamma_k}\kappa_k + \sigma\gamma_k\right)\psi_k \\ \frac{\partial}{\partial z} &= \frac{1}{2}\left(\partial_1 - i\partial_2\right),\ z = x_1 + ix_2 \end{aligned} \tag{5}$$

The formulas (2) and (5) give the expressions for elastic displacements in the shell in terms of the functions φ_k, ψ_k, and φ_k (vortex solution) describes a rotation of an element about the axis $0x_3 : \partial_2 u_{1k} - \partial_1 u_{2k} = \sigma\Delta\varphi_k$.
The integral representations of the functions θ_k, φ_k and ψ_k, coordinated among themselves according to the relations (3) and (4), are taken in the form:

$$\theta_k(z) = \sum_{j=1}^{2}\int_{L_j} p_{jk}\left(\zeta_j\right)K_0\left(\gamma_k r_j\right)ds_j + \frac{2}{\gamma_k}Re\int_{L_j} q_{jk}\left(\zeta_j\right)\frac{\partial}{\partial\zeta_j}K_0\left(\gamma_k r_j\right)d\zeta_j \tag{6}$$

$$\begin{aligned} i\varphi_k(z) - \psi_k(z) &= \sum_{j=1}^{2}\frac{2i}{\gamma_k}\int_{L_j}\overline{q}^{*}_{jk}\left(\zeta_j\right)\frac{\partial}{\partial\overline{\zeta}_j}K_0\left(\gamma_k r_j\right)d\overline{\zeta}_j + \\ &+ \frac{1}{2\gamma_k}\int_{L_j} p_{jk}\left(\zeta_j\right)r_j K_1\left(\gamma_k r_j\right)ds_j + \frac{1}{\gamma_k^2}Re\int_{L_j} q_{jk}\left(\zeta_j\right)\frac{\partial}{\partial\zeta_j}\left(r_j K_1\left(\gamma_k r_j\right)\right)d\zeta_j, \\ r_j &= \left|\zeta_j - z\right|, \quad \zeta_j = \xi_j + i\eta_j \in L_j, \end{aligned}$$

where $K_n\left(\gamma_k r\right)$ is the Macdonald function of the order n, ds – is an arc element of contour L; the densities $p_{jk}\left(\zeta_j\right)$, $q_{jk}\left(\zeta_j\right)$, $q^{*}_{jk}\left(\zeta_j\right)$ are not yet known.
The boundary conditions on the cylindrical surfaces of shell are written in the complex form as follows:

$$\begin{aligned} &\left(\sigma_{11} + \sigma_{22}\right) - e^{2i\psi}\left(\sigma_{22} - \sigma_{11} + 2i\sigma_{12}\right) = 2\left(N - iT\right) \\ &Re\left[e^{-i\psi}\left(\sigma_{13} + i\sigma_{23}\right)\right] = Z \end{aligned} \tag{7}$$

where ψ is an angle between the outward normal to the cylindrical surface and the $0x_1$ axis.

Using Hook's law and the formulas (5), one can represent the conditions (7) in the following form:

$$
\begin{gathered}
2\sigma e^{2i\psi}\left\{\frac{\partial^2}{\partial z^2}\left(i\varphi_k-\psi_k\right)\right\}-\frac{1}{2}\theta_k-\frac{1}{2}\sigma\gamma_k^2\psi_k=\frac{1}{2\mu}\left(N_k-iT_k\right) \\
Re\left\{e^{i\psi}\left[\sigma\gamma_k\frac{\partial}{\partial z}\left(i\varphi_k-\psi_k\right)-\frac{\partial}{\partial z}\left(\sigma\gamma_k\psi_k+\frac{1+\sigma}{\gamma_k}\theta_k\right)\right]\right\}=\frac{1}{2\mu}Z_k
\end{gathered}
\tag{8}
$$

3. The system of singular integral equations

By using the passage to the limit and the representations (6), the boundary value problem (8) is reduced to the following system of six singular integral equations (for each fixed value of k).

$$
\begin{aligned}
&\omega_{12k}a_k+\omega_{13k}b_k+\sum_{j=1}^{2}\sum_{i=1}^{3}\int_{L_j}\omega_{jik}G_{jik}^{(1)}ds_j=\frac{1}{2\mu}\left(N_k^{(1)}-iT_k^{(1)}\right) \\
&\omega_{11k}c_k+\sum_{j=1}^{2}\sum_{i=1}^{3}\int_{L_j}\omega_{jik}G_{jik}^{*(1)}ds_j=\frac{1}{2\mu}Z_k^{(1)} \\
&-\omega_{22k}a_k+\omega_{23k}b_k+\sum_{j=1}^{2}\sum_{i=1}^{3}\int_{L_j}\omega_{jik}G_{jik}^{(2)}ds_j=\frac{1}{2\mu}\left(N_k^{(2)}-iT_k^{(2)}\right) \\
&-\omega_{21k}c_k+\sum_{j=1}^{2}\sum_{i=1}^{3}\int_{L_j}\omega_{jik}G_{jik}^{*(2)}ds_j=\frac{1}{2\mu}Z_k^{(2)}
\end{aligned}
\tag{9}
$$

where:

$$a_k=\frac{\pi i(1+\sigma)}{2\gamma_k},\quad b_k=\frac{\pi(1+\sigma)}{2\gamma_k},\quad c_k=-b_k,$$

$$G_{j1k}^{(n)}\left(\zeta_j,\zeta_{n0}\right)=\frac{\sigma\gamma_k}{4}r_{jn0}K_1\left(\gamma_k r_{jn0}\right)\left(e^{2i\left(\psi_{n0}-\alpha_{jn0}\right)}+1\right)-\frac{1}{2}K_0\left(\gamma_k r_{jn0}\right),$$

$$G_{j2k}^{(n)}\left(\zeta_j,\zeta_{n0}\right)=\frac{\sigma\gamma_k}{4}r_{jn0}K_0\left(\gamma_k r_{jn0}\right)\left[sin\left(\psi_j-\alpha_{jn0}\right)-\frac{ie^{2i\psi_{n0}}}{2}h_{1j}^{(n)}\left(\psi_j,\alpha_{n0}\right)\right]+$$

$$+K_1\left(\gamma_k r_{jn0}\right)\left\{\frac{\sigma}{2}sin\left(\psi_j-\alpha_{jn0}\right)+\frac{ie^{2i\psi_{n0}}}{2}\left[\left(1+\sigma\right)e^{-i\left(\psi_j+\alpha_{jn0}\right)}-\frac{\sigma}{2}h_{2j}^{(n)}\left(\psi_j,\alpha_{in0}\right)\right]\right\},$$

$$G_{j3k}^{(n)}\left(\zeta_j,\zeta_{n0}\right)=\frac{\sigma\gamma_k}{4}r_{jn0}K_0\left(\gamma_k r_{jn0}\right)\left[cos\left(\psi_j-\alpha_{jn0}\right)+\frac{e^{2i\psi_{n0}}}{2}h_{2j}^{(n)}\left(\psi_j,\alpha_{jn0}\right)\right]+$$

$$+K_1\left(\gamma_k r_{jn0}\right)\left\{\frac{\sigma}{2}cos\left(\psi_j-\alpha_{jn0}\right)+\frac{e^{2i\psi_{n0}}}{2}\left[\left(1+\sigma\right)e^{-i\left(\psi_j+\alpha_{jn0}\right)}+\frac{\sigma}{2}h_{1j}^{(n)}\left(\psi_j,\alpha_{jn0}\right)\right]\right\},$$

$$h_{1j}^{(n)}\left(\psi_j,\alpha_{jn0}\right)=e^{i\left(\psi_j-3\alpha_{jn0}\right)}-e^{-i\left(\psi_j+\alpha_{jn0}\right)},$$

$$h_{2j}^{(n)}\left(\psi_j,\alpha_{jn0}\right)=e^{i\left(\psi_j-3\alpha_{jn0}\right)}-e^{-i\left(\psi_j+\alpha_{jn0}\right)},$$

$$G_{j1k}^{*(n)}\left(\zeta_j,\zeta_{n0}\right)=\frac{1}{2}\left[\sigma\gamma_k r_{jn0}K_0\left(\gamma_k r_{jn0}\right)-(1+\sigma)K_1\left(\gamma_k r_{jn0}\right)\right]cos\left(\psi_{n0}-\alpha_{jn0}\right),$$

$$G_{j2k}^{*(n)}\left(\zeta_j,\zeta_{n0}\right)=\frac{\sigma\gamma_k}{4}r_{jn0}K_1\left(\gamma_k r_{jn0}\right)\times\left[sin\left(\psi_{n0}+\psi_j-2\alpha_{jn0}\right)-sin\left(\psi_{n0}-\psi_j\right)\right]-$$

$$-\frac{1}{2}K_0\left(\gamma_k r_{jn0}\right)sin\left(\psi_{n0}-\psi_j\right),$$

$$G_{j3k}^{*(n)}\left(\zeta_j,\zeta_{n0}\right)=\frac{\sigma\gamma_k}{4}r_{jn0}K_1\left(\gamma_k r_{jn0}\right)\times\left[cos\left(\psi_{n0}+\psi_j-2\alpha_{jn0}\right)+cos\left(\psi_{n0}-\psi_j\right)\right]+$$

$$+\frac{1}{2}K_0\left(\gamma_k r_{jn0}\right)cos\left(\psi_{n0}-\psi_j\right),$$

$$q_{jk}^{*}=\frac{i(1+\sigma)}{\sigma\gamma_k^2}q_{jk},\ \omega_{j1k}=p_{jk},\ \omega_{j2k}=Re\,q_{jk},\ \omega_{j3k}=Im\,q_{jk},$$

$$\zeta_j-\zeta_{n0}=r_{jn0}e^{i\alpha_{jn0}},\ \zeta_{n0}=\xi_{n0}+i\eta_{n0}\in L_n.$$

Here ω_{jik} are the unknown densities to be determined.

4. The results and discussion

As an example, let us consider a shell, with the directrices of cylindrical surfaces in the form of an ellipse:

$$L_1:\xi_{11}=R_{11}\cos\varphi_1,\ \xi_{12}=R_{12}\sin\varphi_1,\ 0\le\varphi_1\le 2\pi;$$
$$L_2:\xi_{21}=R_{21}\cos\varphi_2+l_x,\ \xi_{22}=R_{22}\sin\varphi_2,\ 0\le\varphi_2\le 2\pi,$$

Let a load $N=Px_3$ $(P=const)$ be applied on the cylindrical surface with the directrix L_1 and there is no load on the cylindrical surface with the directrix L_2. In the numerical implementation of the developed procedure, the system of integral equations was reduced to the system of linear algebraic equations by the numerical mechanical quadrature method [1, 4].

To characterize the state of stress on the internal cylindrical surface, the following stress was calculated:

$$\sigma_{\theta\theta}=\sigma_{11}\sin^2\theta+\sigma_{22}\cos^2\theta-2\sigma_{12}\cos\theta\sin\theta,$$
$$\theta=\psi-\pi. \tag{10}$$

The numerical procedure of the developed method involves the following steps: at first, the system of the integral equations (9) was solved, then the Fourier coefficients of the stress tensor $\sigma_{ij}^{(k)}$ were determined, and thereafter – unknown stresses on the internal cylindrical surfaces were calculated.

On the Figs. 2-10 the diagrams of the distribution of the relative circumferential stress $\sigma_1=-\sigma_{\theta\theta}/P$ along the internal cylindrical surface are shown:

1) Along the "thickness" coordinate x_3/h at the point where the above stress takes on the maximum value;
2) Along the contour of the directrix of the cylindrical surface.

Numerical results were obtained for Poisson's ratio $\nu = 0.15$. Further, under the approximate solution we will understand the results obtained by the method proposed in this article, and under the exact solution - the solution of the axisymmetric problem, which was obtained by the method of series [13].

Let assume for the definiteness that the contour L_2 is the directrix for the internal cylindrical surface, and L_1 is the directrix for the external cylindrical surface. Let l_x be the distance between the directrix centres, when the above centres are located on the $0x_1$-axis.

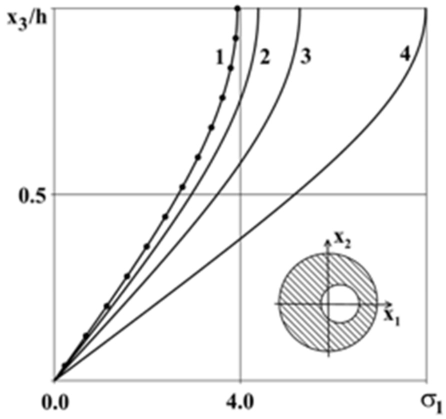

Figure 2. Distribution of the relative circumferential stress over the thickness of the circular shell with the inner circular cylindrical surface

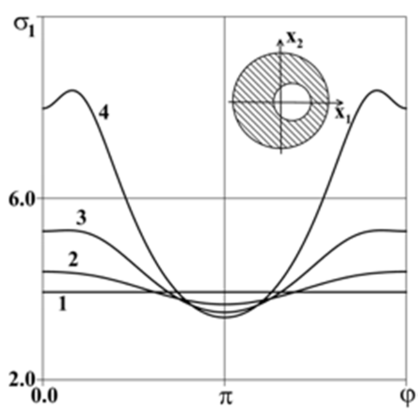

Figure 3. Distribution of the relative circumferential stress along the directrix of the inner circular cylindrical surface for the circular shell

The data given in Figs. 2, 3 refer to the shell with the geometry $R_{11} = R_{12} = 2$, $R_{21} = R_{22} = 1$, $h = 2$.

The curves 1, 2, 3 and 4 (Fig. 2) were constructed along the "thickness" coordinate at the point $\varphi_2 = 0$ for $l_x / R_{21} = 0; 0.25; 0.5; 0.75$ respectively. The points on the curve 1 correspond to the exact solution of the axisymmetric problem. It should be noted a good agreement between the exact and approximate solutions. Fig. 3 shows the distribution of the circumferential stress σ_1 along the directing contour of the cylindrical surface at the section $x_3 / h = 0.98$, which mechanical and geometrical parameters are similar to the curves, shown on the Fig. 2.

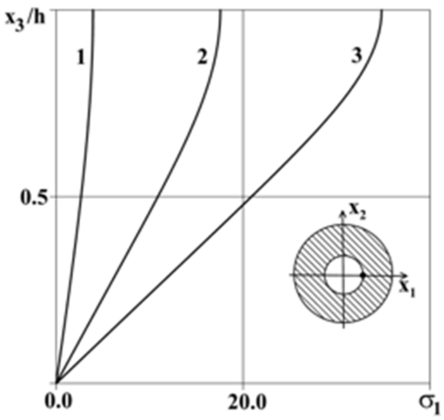

Figure 4. Distribution of the relative circumferential stress over the thickness of the circular shell with the inner circular cylindrical surface

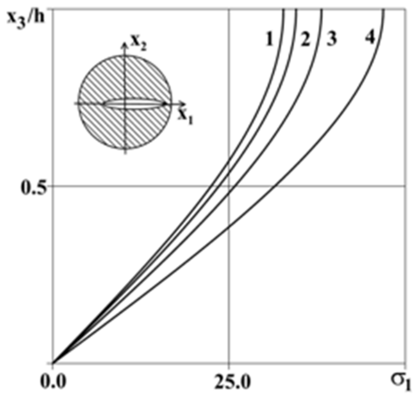

Figure 5. Distribution of the relative circumferential stress over the thickness of the circular shell with the inner elliptic cylindrical surface

The curves 1, 2, 3 (Fig. 4) were constructed for the shell with the following data: $h=2$, $R_{11}=R_{12}=2,$ $R_{21}=R_{22}=1;1.8;1.9$ respectively, at point $\varphi_2=0$ along the "thickness" coordinate. Fig. 5 shows the distribution of the stress σ_1 at the point $\varphi_2=0$ along the "thickness" coordinate of the shell with the following data: $h=2$, $R_{11}=R_{12}=2,$ $R_{21}=1, R_{22}=0.1$. The curves 1-4 were constructed at $l_x=0;0.25;0.50;0.75$ respectively.

Fig. 6 shows the distribution of the stress along the directrix of the cylindrical surface at the section $x_3/h=0.98$. The curves 1, 2, 3 were constructed for the shell with the following data: $h=2$, $R_{11}=R_{12}=2, R_{21}=1,$ $R_{22}=0.1;0.3;0.5$ respectively.

Fig. 7 shows the distribution of the stress σ_1 at the point $\varphi_2=0$ along the "thickness" coordinate of the shell with the following data: $h=2$, $R_{11}=2,$ $R_{12}=1,$ $R_{21}=1, R_{22}=0.1$. The curves 1-4 were constructed at $l_x=0;0.25;0.50;0.75$ respectively.

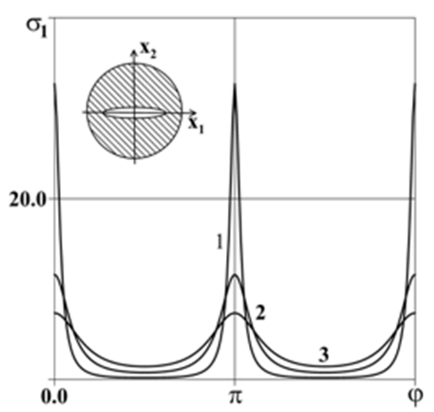

Figure 6. Distribution of the relative circumferential stress along the directrix of the inner elliptic cylindrical surface for the circular shell.

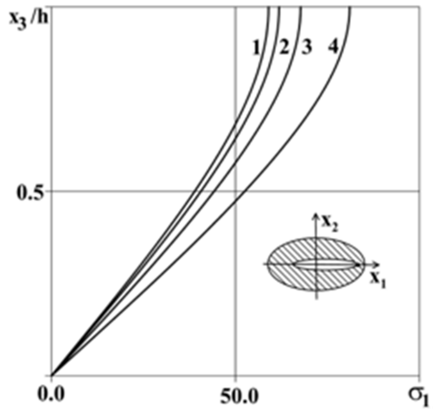

Figure 7. Distribution of the relative circumferential stress over the thickness of the elliptic shell with the inner elliptic cylindrical surface.

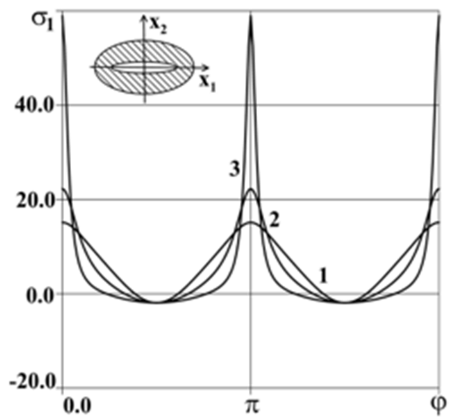

Figure 8. Distribution of the relative circumferential stress along the directrix of the inner elliptic cylindrical surface for the elliptic shell

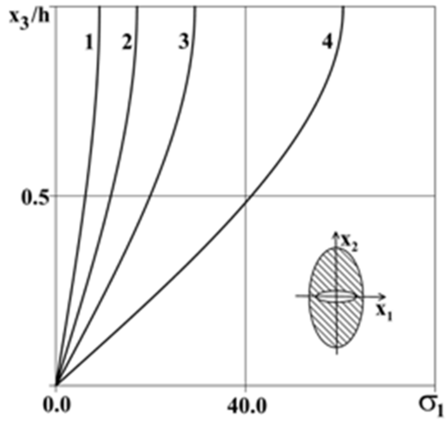

Figure 9. Distribution of the relative circumferential stress over the thickness of the elliptic shell with the inner elliptic cylindrical surface

Fig. 8 shows the distribution of the stress along the directrix of the cylindrical surface at the section $x_3/h = 0.98$. The curves 1, 2, 3 were constructed for the shell with the following data: $h = 2$, $R_{11} = 2,\ R_{12} = 1,\ R_{21} = 1,\ \ R_{22} = 0.5; 0.3; 0.1$ respectively.

Fig. 9 shows the distribution of the stress σ_1 at the point $\varphi_2 = 0$ along the “thickness” coordinate of the shell with the following data: $h=2,\ R_{11} = 1,\ R_{12} = 2,\ R_{22} = 0.1,$ $R_{21} = 0.3; 0.5; 0.7; 0.9$; respectively.

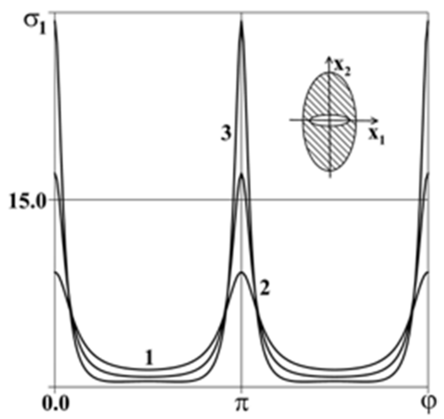

Figure 10. Distribution of the relative circumferential stress along the directrix of the inner elliptic cylindrical surface for the elliptic shell.

Fig. 10 shows the distribution of the stress along the directrix of the cylindrical surface at the section $x_3/h = 0.98$. The curves 1, 2, 3 were constructed for the shell with the following data: $h = 2$, $R_{11} = 1,$ $R_{12} = 2,$ $R_{22} = 0.1;$ $R_{21} = 0.3;0.5;0.7$; respectively.

5. Conclusions

Based on the conducted numerical investigations, the following conclusions can be made:

1. A growth of the relative circumferential stress occurs as the intercentral distance l_x increases.
2. A decrease of the circle shell thickness produces the sharp increase of the relative circumferential stress.
3. For the inner cylindrical surface of circular or elliptic cross sections, the maximum value of the relative circumferential stress takes on the maximum value at point $\varphi_2 = 0\,(\pi)$ for $l_x = 0$. If the inner cylindrical surface is displaced above the mentioned geometries $(l_x > 0)$, the maximum value of the relative circumferential stress shifts along the inner directrix. The actual value of φ_2 where the maximum of the relative circumferential stress will occur depends upon the geometry of the shell, materials from which it is manufactured, as well as upon the applied loading.
4. Comparison of results obtained with the use of the developed procedure and the series method illustrates a sufficiently good convergence of the proposed algorithms and reliability of the numerical results based on these algorithms. The deviation between the above-mentioned approximate and exact results was not more than 2%. This provides a way to apply the proposed procedure to the analysis of the stressed state of a thick-walled shell with a sliding sealing of its ends containing an inclusion made from another material and (or) weakened by a through-thickness cut having sufficiently arbitrary cross sectional geometry.

REFERENCES

1. BELOTSERKOVSKY S.M., LIFANOV I.K.: Method of Discrete Vortices, CRC Press, Boca Raton, 1993.
2. CHEN R., XUE S., CHEN Z., CHEN J.: The numerical solutions of Green's functions for transversally isotropic elastic strata, Applied Mathematics and Mechanics, 21(2000), 49–58.
3. CHUNG Y.-L., PON C.-F.: Boundary element analysis of cracked film-substrate media, International Journal of Solids and Structures, 38(2001), 75–90.
4. ERDOGAN G.D., GUPTA T.S., COOK T.S.: The numerical solutions of singular integral equations, In: Method of Analysis and Solutions of Crack Problems. Noordhoff International Publishing, Leyden, 1973, 268-425.
5. FIL'SHTINSKII L.A.: Periodical solutions of some elastic and electrostatic problems for a cylinder in R3, Theoretical and Applied Mechanics, 21(1990), 13-20 (in Russian).
6. FIL'SHTINSKII L.A., KOVALEV YU.D.: Mixed antisymmetric problem of an elastic layer weakened by through cavities, Materials Science, 37(2001)5, 833-837.
7. FIL'SHTINSKII L.A., KOVALEV YU.D., VENTSEL E.S.: Solution of the elastic boundary value problems for a layer with tunnel raisers, International Journal of Solids and Structures, 39(2002), 6385-6402.
8. FIL'SHTINSKII L.A., KOVALEV YU.D., VENTSEL E.S.: Bending of layers weakend by cuts, International Journal of Solids and Structures, 43(2006), 346-356.
9. FIL'SHTINSKII L.A., KOVALEV YU.D., VENTSEL E.S.: Equilibrium of layers weakened by loaded cuts, International Journal of Solids and Structures, 47(2010), 1490-1495.
10. GRIGOLUK E.I., KOVALEV YU.D.,, FIL'SHTINSKII L.A.: The bending of a semi-layer weakened by through-thickness opening, Rep. Rus. Acad. Sci. 345(1995), 54-56 (in Russian).
11. GRIGORENKO Y.M., KRIKOV N.N., KRIZHANOVSKAYA T.V.: An investigation of stress state of orthotropic hollow cylinders in unsymmetrical loading, Theoretical and Applied Mechanics, 33(2001), pp. 3-6 (in Russian).
12. GRINCHENKO V.T., ULITKO A.F.: An exact solution of the Kirsch problem, International Applied Mechanics 6(1970)5, 455-461.
13. KOSMODAMIANSKII A.S., SHALDYRVAN V.A.: Thick Multiply Connected Plates, Nauk. Dumka, Kiev, 1978, (in Russian).
14. KOVAL'OV YU.D.: Symmetric elasticity problem for a layer with tunnel cavities covered with a diaphragm, Materials Science 38(2002)6, pp. 809-813.
15. LEISSA A.W., QATU M.S.: Vibrations of continuous systems, New York: Mc Graw Hill, 2011.
16. LIFANOV I.K.: Singular integral equations and discrete vortices, VSP, Utrecht, The Netherland, 1996.
17. LUR'YE A.I.: To the theory of thick plates, Prikl. Mekh. Matem. 6(1942), 151-168 (in Russian).
18. MATYSIAK S.J., PAUK V.J.: On crack problems in an elastic ponderable layer, International Journal of Fracture. 96(1999)4, 371–380.

19. MESHII T., WOCTANABE K.: Simplified equations to evaluate the stress intensity factor of an arbitrarily located circumferential crack in a finite cylinder under axisymmetric bending, Nikon Kikai Gakkai Ronbunshu, A (Trans. Jpn. Soc. Mech. Eng. A) 625(1998), 2361-2366.
20. NODA N.-A., TOMARI H., MATSUO T.: Interaction effect between ellipsoidal inclusions in an infinite body under asymmetric uniaxial tension, Nikon Kikai Gakkai Ronbunshu, A (Trans. Jpn. Soc. Mech. Eng. A) 622(1998), pp. 1577–1582.
21. SIH G.C., WILLIAMS M.L., SWEDLOW J.L.: Three dimensional stress distribution near a sharp crack in a plate of finite thickness, AFML, Wright-Patterson Air Force Base, AFML-TR-66-242, 1966
22. SUNDARA RAJA IYENGAR K.T., MURTHY M.V.V, BAPU RAO M.N.: Three dimensional elastic analysis of cracked thick plates under bending fields, International Journal of Solids and Structures, 24(1988), 683–703.